Experimental evidence for a dynamical crossover in liquid aluminium

2015 J. Phys.: Condens. Matter 27 455102

(http://iopscience.iop.org/0953-8984/27/45/455102)

IOP Publishing Journal of Physics: Condensed Matter
J. Phys.: Condens. Matter **27** (2015) 455102 (6pp) doi:10.1088/0953-8984/27/45/455102

Experimental evidence for a dynamical crossover in liquid aluminium

F Demmel[1], A Fraile[2,3], D Szubrin[4], W-C Pilgrim[4] and C Morkel[5]

[1] ISIS Facility, Rutherford Appleton Laboratory, Didcot OX11 0QX, UK
[2] CCQCN, Department of Physics, University of Crete, Heraklion, Greece
[3] Instituto de Fusion Nuclear, Universidad Politecnica de Madrid, Jose Gutierrez Abascal 2, 28006 Madrid, Spain
[4] Fachbereich Chemie, Philipps-Universität Marburg, 35032 Marburg, Germany
[5] Physikdepartment E21, TU München, 85748 Garching, Germany

E-mail: franz.demmel@stfc.ac.uk

Received 16 June 2015, revised 28 August 2015
Accepted for publication 16 September 2015
Published 14 October 2015

Abstract

The temperature dependence of the dynamic structure factor at next-neighbour distances has been investigated for liquid aluminium. This correlation function is a sensitive parameter for changes in the local environment and its Fourier transform was measured in a coherent inelastic neutron scattering experiment. The zero frequency amplitude decreases in a nonlinear way and indicates a change in dynamics around $1.4 \cdot T_{\mathrm{melting}}$. From that amplitude a generalized viscosity can be derived which is a measure of local stress correlations on next-neighbour distances. The derived generalized longitudinal viscosity shows a changing slope at the same temperature range. At this temperature the freezing out of degrees of freedom for structural relaxation upon cooling sets in which can be understood as a precursor towards the solid state. That crossover in dynamics of liquid aluminium shows the same signatures as previously observed in liquid rubidium and lead, indicating an universal character.

Keywords: liquid metals, dynamics, neutron scattering

(Some figures may appear in colour only in the online journal)

1. Introduction

The liquid state is limited by first order transitions to a crystalline state or at high temperature to the gas. Cooling down a liquid at ambient pressure all except Helium attain a solid state. If a crystalline state is reached a dramatic change in long range order occurs manifesting the first order phase transition. However, if crystallization can be avoided the liquid can be undercooled and eventually the material morphs into a glass. From structural point of view the liquid and glass state do not differ very much [1]. Yet the dynamics changes dramatically towards the glass transition. Viscosity increases many orders of magnitude in a small temperature range and concomitant the structural relaxation process slows down [2]. Structural degrees of freedom freeze out towards the calorimetric glass temperature T_{g}, which is defined when the viscosity reaches a certain limit and structural relaxation times become macroscopic. The melting temperature T_{m} has no significance for the changes in dynamics into the glass state [3]. A lot of effort has been devoted to establish the changes in dynamics towards the glass transition in the past. Less simple to answer is the question at which temperature that slowing down sets in or whether such a temperature range exists at all. Here we present evidence for significant changes in dynamics of liquid aluminium at about $1.4 \cdot T_{\mathrm{m}}$ (T_{m} is the melting temperature) which can be understood as a precursor to structural freezing.

The dynamics of a dense liquid shows reminiscences from the solid state. For example, in simple liquid metals well defined acoustic excitations exist, resembling the acoustic phonons in the crystal (see for a more recent review [4]). Even the quintessence of the liquid state, the viscosity, can be circumvented by a quick time probe. Then the liquid reacts like a solid, which is known as a visco-elastic response, and propagating transverse excitations are predicted [5, 6] and have been demonstrated by molecular dynamics simulations [7]. A large amount of experimental studies on liquid metal dynamics

have been conducted near the melting point, but only a few followed and revealed subtle changes in liquid dynamics with rising temperature, see e.g. [8, 9].

Coherent neutron scattering provides insight into the collective movements of the particles. In the hydrodynamic limit the scattering function is given by a combination of three Lorentzians, neglecting a small asymmetry term [10]. The Brillouin lines disperse with the velocity of sound and can be followed far into the microscopic region [4]. For larger momentum transfers or when length scales of atomic diameters are probed the quasielastic line shows a narrowing around the structure factor maximum, known as deGennes narrowing [11]. In the time domain the intermediate scattering function for density fluctuations $F(Q, t)$ demonstrates a slowing down at the structure factor maximum. In a simple picture it costs time for a density fluctuation to relax on a next-neighbour length scale due to a necessary rearrangement of the surrounding particles. That necessary time cost appears in the frequency domain as a narrowing of the quasielastic line. On this length scale the most direct access to the evolution of structural relaxation is provided. MD-simulations on liquid rubidium revealed a further slow process within that relaxation process which has been described by mode coupling theory quantitatively and can be regarded as a precursor to structural freezing [12].

Aiming to reveal reminiscences of the solid state in the liquid dynamics, our measurements focus on relaxation processes at nearest neighbour length scales. Changes on the local structural relaxation of density fluctuations due to cooling will be monitored very precisely with that amplitude at zero energy transfer. That relaxation process is inherently linked to a collective rearrangement of the nearest neighbour particles in a dense fluid and hence is best observed in a coherent scattering experiment. A distinct change in the amplitude might be related to a further relaxation process. Hence the study of $S(Q, \omega = 0)$ allows to monitor changes in the relaxation dynamics of the intermediate scattering function. For example, the onset of a further slow exponential decay process will appear directly in the amplitude $S(Q, \omega = 0)$, which can be understood from the Fourier transform relationship between $F(Q, t)$ and $S(Q, \omega = 0)$. Furthermore, the amplitude at zero energy transfer is related to a generalized longitudinal viscosity, which will provide insight into the evolution of stress correlations with rising temperature on next neighbour distances.

Previously we measured the temperature dependence of the line width at the structure factor maximum of the alkali metal rubidium [13] and liquid lead [14]. The derived amplitude at energy transfer zero demonstrates a change with increasing temperature. The amplitude drops twice as fast between melting point and 1.5 T_m than between 1.5 T_m and 2 T_m in both cases. In addition, the derived Q-dependent longitudinal viscosity shows a decrease at the same temperature range with increasing temperature. These facts might be interpreted that the liquid metal behaves more solid-like on cooling starting at a temperature $T \approx 1.5\ T_m$. A more detailed investigation into the relaxation dynamics of liquid rubidium revealed a slow structural relaxation process near the melting point, related to structural freezing [15]. Following that relaxation with rising temperature demonstrated that the slow structural relaxation seems to disappear at $T \approx 1.3\ T_m$. That temperature range between $T \approx 1.3\ T_m$ and $T \approx 1.5\ T_m$ appears to be the onset of a slow structural relaxation process which eventually, if crystallization can be avoided, ends in the glassy state. Interestingly a quite recent MD-simulation on a molten metallic alloy suggested a dynamical crossover in a similar temperature range [16].

Here we present a similar change in dynamics in liquid aluminium. Aluminium has a different valence than rubidium or lead and the interatomic potential derived from pseudopotential theory is significant different [17, 18]. Aluminium presents therefore an important example for a supposed universal character of the dynamical changes in liquid metals. Despite the differences in interaction potential a hard sphere model provides a fair description of the structure factor of liquid aluminium [19]. Most of the scattering experiments on liquid aluminium have until now focused on the structure and dynamics near the melting point [20–23]. Recently we have investigated the diffusion behavior of liquid aluminium with increasing temperature up to $T = 1.2 \cdot T_m$ [24]. Now we demonstrate changes in next-neighbour dynamics in a wide temperature range up to $T \approx 1.7\ T_m \approx 1600$ K.

2. Experimental details

Aluminium is a pure coherent scatterer with an incoherent cross section of less than 0.01 barn compared to the coherent cross section of 1.495 barn. Because aluminium builds an alloy with almost all metals alumina was chosen as sample can material. The same cell material was used in an early structure factor measurement [20]. A cylindrical cell with an outer diameter of 25 mm and an inner diameter of 20 mm was filled with a 99.999% pure aluminium rod. The alumina cell was closed with a niobium cap glued onto the alumina cell by a ceramic high temperature glue. The sample was installed in a furnace and heated with a stability of ± 2 K. The melting point of aluminium is 933.5 K. Measurements have been performed between the melting point and 1593 K in about 50 K steps. The measurement time varied between 5 and 12 h per temperature. The spectra of liquid aluminium have been measured at the IRIS-spectrometer of the ISIS Facility, UK. A spectrometer configuration with an end energy of 7.38 meV was chosen, which provided an energy resolution of 0.055 meV (FWHM). This good energy resolution well separated from the liquid aluminium dynamics facilitates the correction of the empty can contribution. The Q-resolution was about ± 0.04 Å^{-1}. The structure factor maximum of liquid aluminium occurs at $Q_0 = 2.7$ Å^{-1} and the peak position does not shift within the Q-resolution and within the investigated temperature range. A strong powder line of solid alumina occurs at $Q = 3$ Å^{-1} and a weaker line at $Q = 2.45$ Å^{-1} and hence they will not interfere with the data analysis at the structure factor peak of liquid aluminium. The data analysis included

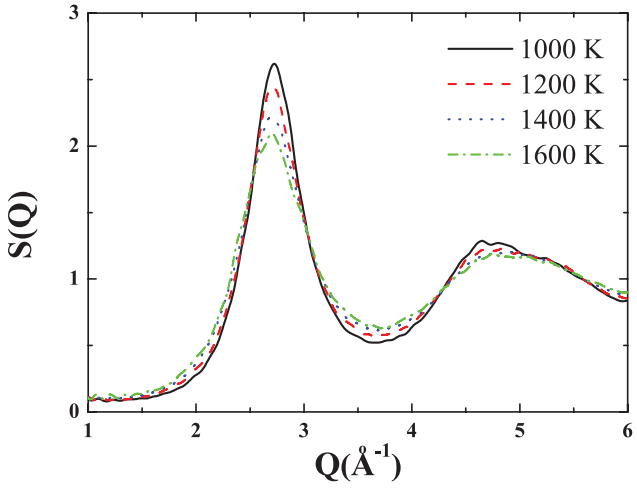

Figure 1. The structure factor $S(Q)$ from the simulation is plotted for four temperatures.

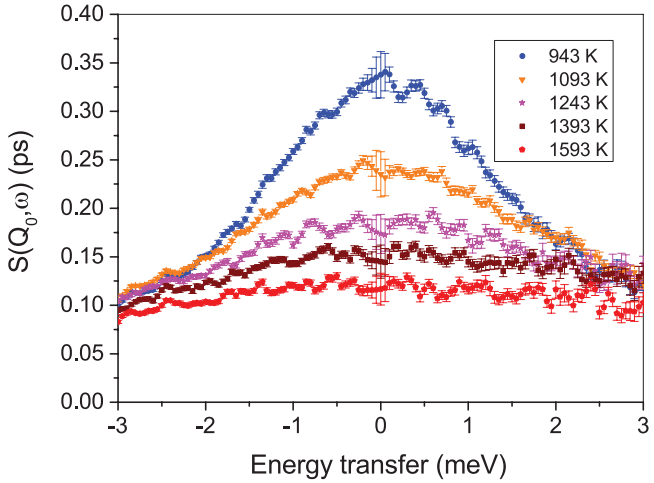

Figure 2. Spectra at five temperatures of liquid aluminium are depicted for $Q_0 = 2.7$ Å^{-1} at the peak of the structure factor. Due to the transformation from time of flight to energy the statistics gets worse at positive energy transfers.

monitor normalisation, empty cell subtraction and conversion into constant Q-spectra. Absorption coefficients for the empty cell subtraction have been calculated according to a method of Paalman and Pings [25]. Within a Monte Carlo procedure averaged absorption factors for crossing the can and/or sample are calculated. These factors are typically between 0.65 and 0.75 and only weakly energy dependent or scattering angle dependent due to the cylindrical geometry. If necessary a scaling factor between 0.85 and 0.9 was used to subtract completely the elastic line contributions of the can. Finally a constant energy bin size of 0.05 meV was applied to the spectra. A linear sloping background probably reasoned by higher order reflections at the analyzer crystals was subtracted from the spectra. The multiple scattering contribution is small at the structure factor maximum and was not corrected. By comparison with a vanadium scatterer an absolute calibration of the spectra was achieved. To extract the amplitude without ambiguity a fit with a single Lorentzian function convoluted with the resolution function was applied.

3. MD simulations

To support the analysis of the experimental data MD-simulations have been performed by means of Embedded Atom Method (EAM) potentials. The aim of the simulations was to extract a set of consistent structure factor data over the whole experimental covered temperature range. The EAM method is a commonly used representation for the energy that overcomes the volume dependent limitation of pair-potentials by adding a term for the energy to embed an atom in the background electron density of its neighbours [26]. Most of the EAM potentials were originally proposed for solid-state calculations, however these potentials have often been found to successfully describe the thermodynamics and transport properties of liquid metals in several systems, like Cu, Ag, Au, Ni, Pd, and Pt [27] and Li, Pb and LiPb alloys [28]. Here we made use of the new EAM angular dependent potential (ADP) developed by Apostol and Mishin [29]. The cutoff for the Al–Al interaction potential is 6.287 Å. Simulation runs were performed on 13 500 atoms. Periodic boundary conditions were imposed to minimize surface and edge effects and size effects have been tested. MD simulations were carried out using the parallel code LAMMPS [30]. The integration time step Δt used for the heating, equilibrating and production phases was $5 \cdot 10^{-5}$ ps. Average length of simulation time in production stage (equilibrium) was around 50 ps. Trajectories in the canonical ensemble (NVT) were generated after 25 ps of heating by coupling our system to a Berendsen thermostat and ulterior equilibration and production phases by means of a Nose–Hoover thermostat-barostat [31].

The MD simulations were conducted in cooling mode, i.e. the sample is heated up to a temperature well above the melting temperature and then equilibrated at the desired temperature, ensuring that the sample is in liquid phase. Then production runs were simulated in the isothermal-isobaric (NPT) ensemble. The simulated density was about 3% larger than the experimental density for all temperatures. Physical and structural properties have been calculated in the last 2 ps production phase of each MD trajectory, averaging up to 10 runs starting from different initial conditions, for 8 temperatures between melting point and 1600 K. The simulation results for the structure correspond very well to MD-simulations results based on EAM potentials from Becker and Kramer [32]. In figure 1 we show structure factors $S(Q)$ of liquid aluminium from the simulation with rising temperature. They demonstrate that the peak value $S(Q_0)$ decreases, however the peak position does not shift within that temperature range.

4. Results and discussion

In figure 2 five spectra at $Q_0 = 2.7$ Å^{-1} are displayed. The amplitude is given in absolute units and compares fairly well with results from early MD simulations [17] and theoretical calculations [33]. The increased error bars near zero energy transfer stem from the alumina can subtraction, which does not affect the following analysis because the energy resolution is

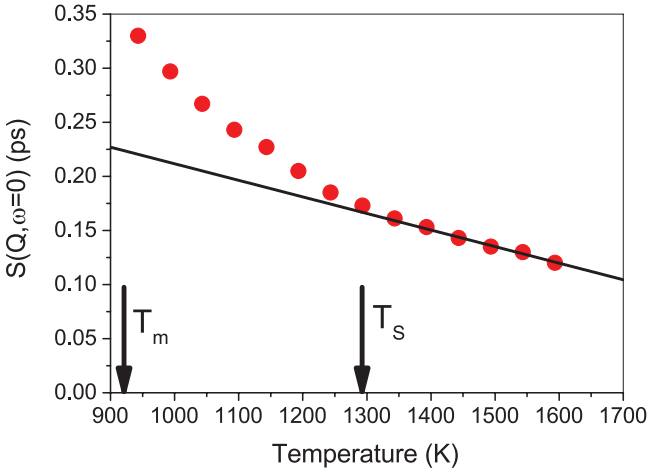

Figure 3. The amplitudes $S(Q_0, \omega = 0)$ are shown. Error bars are smaller than symbols. As a guide to the eye a linear fit through the high temperature points is included. T_m denotes the melting temperature and T_S a high temperature stability limit for the solid state from thermodynamical calculations [42].

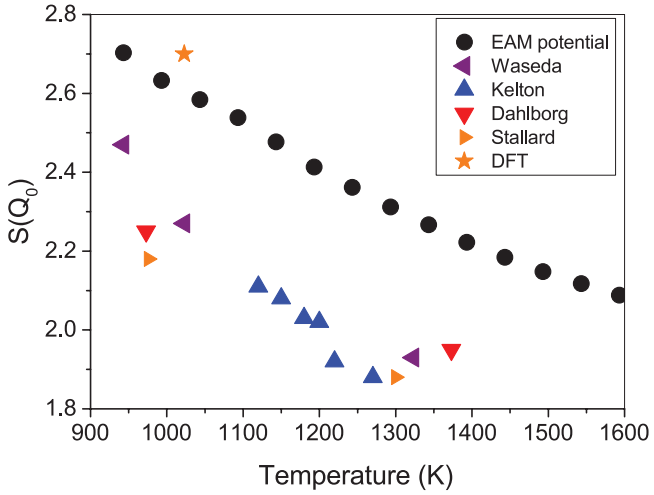

Figure 4. Peak values $S(Q_0)$ of liquid aluminium are plotted from experiments and simulations. *Waseda* from [36], *Dahlborg* from [37], *Stallard* from [20], *Kelton* from [21] and *DFT* from [38].

more than an order of magnitude smaller than the dynamics of aluminium. Clearly visible is the change of amplitude at zero energy transfer, when up to 1293 K the amplitude is reduced about twice the amount compared to the change up to 1593 K. With increasing temperature the spectra broaden and extend beyond the available dynamic range of the spectrometer. That broadening of the spectra prevents extracting directly structure factor data from the experiment. Figure 3 depicts the extracted amplitudes $S(Q_0, \omega = 0)$. With increasing temperature the amplitude decreases in a continuous but nonlinear manner. This was emphasized through a linear fit through the temperature points above 1293 K. Such a linear fit has no theoretical basis and is merely a guide to the eye. However, there is obviously a change in the slope around $T \approx 1300$ K. Because we are probing structural relaxations at nearest neighbour distances that change in dynamics is evidence for a change in dynamics. The difference between the amplitude at low temperature and the linear extrapolated high temperature amplitude might be understood with a further slow relaxation process.

The amplitude $S(Q, \omega = 0)$ is connected to a generalized longitudinal viscosity coefficient $\eta_l(Q)$ according to [34]:

$$\eta_l(Q) = \pi \rho v_0^2 \frac{S(Q, \omega = 0)}{S(Q)^2} \qquad (1)$$

with v_0 the thermal velocity and ρ the mass density. The generalized longitudinal viscosity $\eta_l(Q)$ is the zero frequency limit of the Q-dependent autocorrelation function of the diagonal elements of the microscopic stress tensor [6]. The longitudinal viscosity is a measure for the diffusion of momentum parallel to the velocity of the particles and can be regarded as being sensitive to long lasting atomic-level stress correlations, in our case, on next neighbour distances. In equation (1) $\eta_l(Q_0)$ is linked with three parameters, which are all temperature dependent: the square of the thermal velocity increases linearly with temperature, the mass density decreases with temperature [35] and the structure factor $S(Q)$ does the same.

To obtain reliable and consistent $S(Q_0)$ data over a wide temperature range is not trivial. We searched the literature to asses the published $S(Q)$ data. In figure 4 we compare experimental and computational results for $S(Q_0)$.

Experimental data are available from x-ray scattering for three temperatures: 943 K, 1023 K and 1323 K [36]. More recently synchrotron data have been published by Kelton *et al* in a temperature range between 1100 K and 1280 K [21]. Two temperatures have been published from neutron diffraction [20, 37]. Unfortunately there are no data published for higher temperatures. That uncertainty in experimental values calls for input from simulations. Included in the figure are the $S(Q_0)$ values from our EAM simulation interpolated to the temperatures of the experiment. Clearly the simulated values are lying above all available experimental values. However, the simulation values agree quite well with published simulation results using different implementations of EAM potentials [32]. A first principles based simulation obtained a similar large $S(Q_0)$ value [38] for liquid aluminium near the melting point. That good agreement between simulations, classical or first-principles based, convinced us to use the structural data from the EAM simulation, even though there is a systematic offset to experimental data. In table 1 the experimental densities of liquid aluminium and the interpolated $S(Q_0)$ values from the simulation are listed.

Taking the simulated $S(Q_0)$ values into equation (1) we obtain the generalized viscosities shown in figure 5 in absolute units. Although there appear three parameters with different temperature dependencies in equation (1) we obtain a change in the slope of the viscosity around 1300 K. Jakse and Pasturel have recently calculated the generalized shear viscosity $\eta_s(Q)$ of liquid aluminium from *ab initio* based molecular dynamics simulations [39]. They obtain values $\eta_s(Q_0)$ compatible with our $\eta_l(Q_0)$ values. Included in the figure are the experimental values for the macroscopic shear viscosity, which are known up to about 1300 K [35]. Unfortunately there are no data at

Table 1. The experimental densities [35] and the $S(Q_0)$ values from the EAM ADP simulation are presented.

Temperature (K)	density (g cm^{-3})	$S(Q_0)$
943	2.375	2.703
993	2.345	2.63
1043	2.331	2.58
1093	2.314	2.54
1143	2.297	2.48
1193	2.279	2.41
1243	2.261	2.36
1293	2.244	2.31
1343	2.226	2.26
1393	2.209	2.22
1443	2.192	2.18
1493	2.274	2.15
1543	2.156	2.12
1593	2.139	2.09

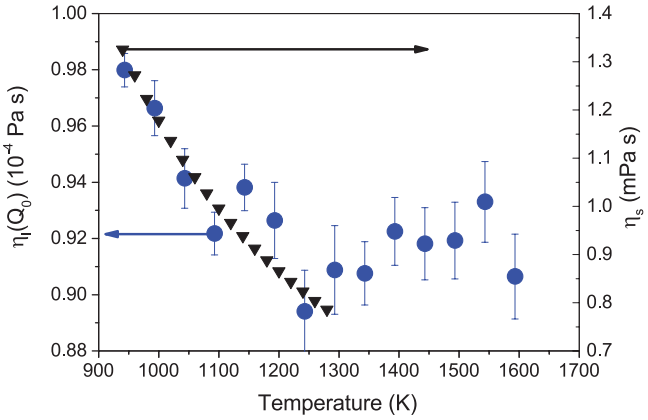

Figure 5. The generalized viscosity $\eta_l(Q_0)$ (circles) is plotted obtained from equation (1). The error bars are derived from the uncertainty in determining the amplitude $S(Q_0, \omega = 0)$. Included are experimental values for the macroscopic shear viscosity (triangles) [35].

higher temperatures published, but we suppose that there is a smooth decrease with further increasing temperature as it was observed for example in liquid lead [14]. In contrast, the Q-dependent viscosity demonstrates a different behaviour and starts to increase around 1300 K coming from high temperature. Increase in the autocorrelations of the stress tensor is a sign of a more solid-like behaviour. That increase in generalized viscosity and the increase of the amplitude $S(Q_0, \omega = 0)$ can be interpreted that the liquid metal dynamics changes to a more solid-like behaviour. A similar abrupt change in the generalized viscosity was observed for liquid rubidium and liquid lead [13, 14]. In addition, a sophisticated calculation of generalized viscosities at the structure factor maximum from a liquid rubidium MD-simulation demonstrated a similar increase with decreasing temperature [40].

Egami and coworkers have studied a model of liquid iron through MD-simulations in the past [41]. They derived atomic level shear stress correlations from their data over a wide range of temperatures. At a temperature range of about twice the glass temperature T_g they observed an increase of the local stress correlations upon cooling. No experimental

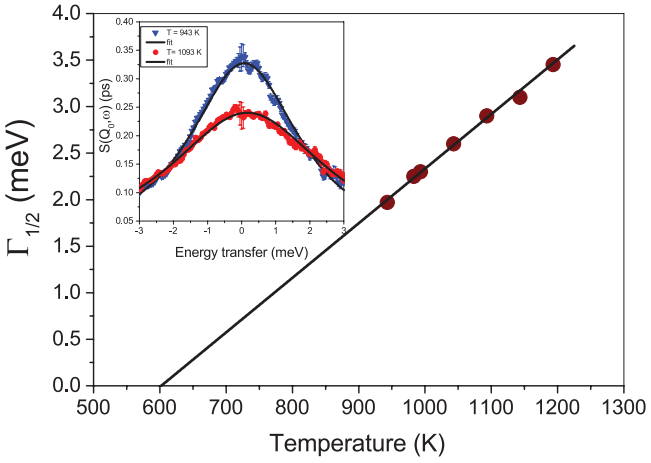

Figure 6. The half width at half height from a Lorentzian fit to the spectra at the structure factor maximum of liquid aluminium is plotted. Note that the error bars from the fits are smaller than the symbol size. Included is a linear fit through the data points which is extrapolated to zero line width. The inset shows two spectra with the respective fits of a Lorentzian line to extract the linewidth.

data for the glass temperature T_g of aluminium is available to our best knowledge. For an estimate we used our previous data where we investigated the line width of the deGennes narrowing, a process related to a self diffusion process [24]. Figure 6 shows the half width at half maximum of liquid aluminium at the structure factor maximum. A simple estimate for the temperature when structural relaxation has ceased can be obtained from these widths by a linear extrapolation to zero energy width. That extrapolation indicates a T_g for aluminium of about 600 K. Empirically it was found that $T_g \approx 2/3\, T_m$ for many glass formers [2], which agrees quite well with our estimate. We conclude that the observed changes in dynamics in liquid aluminium are compatible with a value of twice of T_g and hence with the predictions of Egami and coworkers for an iron model. That agreement and the similar changes observed in liquid rubidium and liquid lead might evidence an universal crossover in liquid metal dynamics. Quite recently a MD-simulation on metallic alloys reported a crossover phenomenon roughly at twice the glass transition temperature of the system [16]. That observation was based on self-diffusion and shear viscosity investigations. This report based on a glass forming metallic alloy seem to agree perfectly with our experimental observations.

There is also some support for our findings from thermodynamics. Some time ago the thermodynamics of aluminium has been studied over a wide temperature range [42]. If heterogenous melting can be avoided, at for example grain boundaries or free surfaces, a crystal can be superheated. Eventually the entropy of the hot crystalline state will exceed the liquid one and the crystal will melt. Such a stability limit has been predicted for aluminium with a stability limit temperature $T_S = 1.38\, T_m$. In a later MD-simulation on superheating of aluminium crystals a solid to liquid transition at $T_S = 1.3\, T_m$ was observed [43]. Vice versa that temperature can be regarded as the highest temperature up to which solidstate-like structures might survive. That temperature range agrees fairly well with the temperature

range where our measurements indicate a change to a more solid-like behaviour in the liquid state (see figure 3).

5. Conclusion

We performed quasielastic neutron scattering experiments on liquid aluminium up to $T = 1600$ K. The experiments focused on the changes in dynamics at the structure factor maximum. The amplitude at zero frequency shows a changing slope with increasing temperature at $T \approx 1.4\,T_{\mathrm{m}}$. That change in slope can be understood that upon cooling a further relaxation process sets in. With the help of EAM simulations the generalized longitudinal viscosity could be derived. This quantity shows an increase with decreasing temperature in the same temperature range $T \approx 1.4\,T_{\mathrm{m}}$. Such a behaviour can be interpreted as an onset of more solid-like dynamics in the liquid state upon cooling. Thermodynamic calculations for the solid state predicted an upper temperature stability limit for the solid phase which corresponds favorable with our observations. We conclude that liquid aluminium shows a dynamical crossover from a liquid state to a dense viscous liquid state around $T \approx 1.4\,T_{\mathrm{m}}$, which marks the onset of slowing down in structural relaxation towards the glass transition. Remarkably a very similar temperature for a dynamical crossover was found in a MD-simulation on a metallic alloy quite recently [16]. That crossover, experimentally observed also in rubidium and lead, might be universal to liquid metals and even alloys. Beyond the interest to understand the fundamental processes of solidification the identification of precursor processes to freezing of metals and alloys might have technological implications for casting and welding.

Acknowledgments

We thank the ISIS Facility for the provision of beam time and the Furnace section for the excellent support. This work was partially supported by the European Union's Seventh Framework Programme (FP7-REGPOT-2012-2013-1) under grant agreement no 316165 and by the Science and Technology Facilities Council, STFC.

References

[1] Berthier L and Biroli G 2011 *Rev. Mod. Phys.* **83** 587
[2] Debenedetti P G and Stillinger F H 2001 *Nature* **410** 259
[3] Götze W 2009 *Complex Dynamics of Glass-Forming Liquids* (Oxford: Oxford University Press)
[4] Scopigno T, Ruocco G and Sette F 2005 *Rev. Mod. Phys.* **77** 881
[5] Egelstaff P A 1992 *An Introduction to the Liquid State* (Oxford: Clarendon Press)
[6] Hansen J P and McDonald I R 2006 *Theory of Simple Liquids* (London: Academic)
[7] Levesque D, Verlet L and Kurkijarvi J 1973 *Phys. Rev.* A **7** 1690
[8] Morkel C, Gronemeyer C, Gläser W and Bosse J 1987 *Phys. Rev. Lett.* **58** 1873
[9] Pilgrim W-C, Ross M, Yang L H and Hensel F 1997 *Phys. Rev. Lett.* **78** 3685
[10] Boon J P and Yip S 1980 *Molecular Hydrodynamics* (New York: McGraw Hill)
[11] deGennes P G 1959 *Physica* **25** 825
[12] Balucani U and Vallauri R 1989 *Phys. Rev.* A **40** 2796
[13] Demmel F, Diepold A, Aschauer H and Morkel C 2006 *Phys. Rev.* B **73** 104207
[14] Demmel F, Howells W S and Morkel C 2008 *J. Phys.: Condens. Matter* **20** 205106
Demmel F, Howells W S, Morkel C and Pilgrim W-C 2010 *Z. Phys. Chem.* **224** 83
[15] Demmel F, Fouquet P, Häussler W and Morkel C 2006 *Phys. Rev.* E **73** 032202
Demmel F and Morkel C 2012 *Phys. Rev.* E **85** 051204
[16] Jaiswal A, Egami T and Zhang Y 2015 *Phys. Rev.* B **91** 134204
[17] Ebbsjo I, Kinell T and Waller I 1980 *J. Phys.* C **13** 1865
[18] Hafner J and Heine V 1983 *J. Phys. F.: Met. Phys.* **13** 2479
[19] Hafner J 1977 *Phys. Rev.* A **16** 351
[20] Stallard J M and Davis C M 1973 *Phys. Rev.* A **8** 368
[21] Mauro N A, Bendert J C, Vogt A J, Gewin J M and Kelton K F 2011 *J. Chem. Phys.* **135** 044502
[22] Scopigno T, Balucani U, Ruocco G and Sette F 2000 *Phys. Rev.* E **63** 011210
[23] Kargl F, Weis H, Unruh T and Meyer A 2012 *J. Phys. Conf. Ser.* **340** 012077
[24] Demmel F, Szubrin D, Pilgrim W-C and Morkel C 2011 *Phys. Rev.* B **84** 014307
[25] Paalman H H and Pings C J 1962 *J. Appl. Phys.* **33** 2635
[26] Daw M S and Baskes M I 1984 *Phys. Rev.* B **29** 6443
Foiles S M 1985 *Phys. Rev.* B **32** 7685
[27] Foiles S M and Adams B 1989 *Phys. Rev.* B **40** 5909
[28] Fraile A, Cuesta-López S, Schwen D, Caro A and Perlado J M 2014 *J. Nucl. Mater.* **448** 103
[29] Apostol F and Mishin Y 2010 *Phys. Rev.* B **82** 144115
[30] Large-scale Atomic/Molecular Massively Parallel Simulator, LAMMPS: http://lammps.sandia.gov
[31] Martyna C J, Klein M L and Tuckerman M 1992 *J. Chem. Phys.* **97** 2635
[32] Becker C A and Kramer M J 2010 *Modelling Simul. Mater. Sci. Eng.* **18** 074001
[33] Sjogren L 1978 *J. Phys.* C **11** 1493
[34] Kugler A A 1973 *J. Stat. Phys.* **8** 107
[35] Assael M J *et al* 2006 *J. Phys. Chem. Ref. Data* **35** 285
[36] Waseda Y 1980 *The Structure of Non-Crystalline Materials* (New York: McGraw Hill)
[37] Dahlborg U *et al* 2013 *J. Non-Cryst. Solids* **361** 63
[38] Rüter H R and Redmer R 2014 *Phys. Rev. Lett.* **112** 145007
[39] Jakse N and Pasturel A 2013 *J. Phys.: Condens. Matter* **25** 285103
Jakse N and Pasturel A 2013 *Sci. Rep.* **3** 3135
[40] Bertolini D, Demmel F and Tani A 2007 *Phys. Rev.* B **76** 094204
[41] Chen S P, Egami T and Vitek V 1988 *Phys. Rev.* B **37** 2440
Tomida T and Egami T 1995 *Phys. Rev.* B **52** 3290
[42] Fecht H J and Johnson W L 1988 *Nature* **334** 50
[43] Forsblom M and Grimvall G 2005 *Phys. Rev.* B **72** 054107